Assessment of a tensile constitutive model considering various loading histories for early age concrete

M. Kunieda, W. Srisoros, N. Ueda & H. Nakamura
Dept. of Civil Engineering, Nagoya University, Nagoya, Japan

Y. Ishikawa
Dept. of Civil Engineering, Meijo University, Nagoya, Japan

ABSTRACT: Flexural tests were carried out under the several loading conditions, to verify a constitutive model subject to both hardening process and loading histories for early age concrete. A method of specifying the shape of a bilinear tension softening curve using a volume function produced from time-dependent changes in various material properties was proposed, with its validity being verified by comparison with test results. Then, a technique of superposing a stress-strain curve specified using the volume function for each time step was analytically verified using the Rigid-Body-Spring Model. This technique roughly reproduced the load-CMOD curves obtained from the tests, proving its validity.

1 INTRODUCTION

Cracking of early age concrete, such as thermal cracking in massive concrete and cracking resulting from drying shrinkage or autogenous shrinkage, not only forms mechanical weaknesses but also causes a reduction in durability. It is therefore important to quantitatively evaluate the cracking properties of early age concrete. The location, length, and width of thermal cracks, for instance, are strongly affected by the time-dependent changes in the mechanical properties and temperature history (corresponding to loading history) of concrete. Quantitative evaluation of stresses generated in concrete until cracking has been progressively practiced in light of the development of numerical analysis techniques incorporating changes in the material properties of concrete after placing (e.g. strength, elastic modulus, and creep behavior). In order to predict the cracking properties of a concrete structure by numerical analysis, it is urgently necessary to develop a constitutive model that is capable of simultaneous quantitative treatment of both (1) time dependency in the mechanical properties of concrete including softening after cracking and (2) differences in the external loading histories acting on concrete.

The authors have been working on the development of constitutive models subjected to the hardening process and loading history of concrete, while conducting various verification analyses (Ishikawa et al. 2005, Srisoros 2006). Comparison with test data and their verification are now required. In this study, flexural tests were conducted under conditions involving different hardening processes and loading histories of concrete to verify the validity of the constitutive model proposed by the authors.

2 OUTLINE OF PROPOSED CONSTITUTIVE MODEL SUBJECTED TO HARDENING PROCESSES AND LOADING HISTORIES

Bazant et al. (1989) proposed the solidification theory to represent time-dependent creep behavior of concrete. In this theory, global response of concrete depends on each solidified element that represents the physical phenomenon at the micro-scale. In addition, the solidification theory proposed by Bazant et al. has the equilibrium condition in force for total volume considering static constraints. However, the constitutive model proposed by the authors characterized with kinematic constraints, in which each solidified element has the same strain increment at each time step. Therefore, calculating the stress at each time step becomes easier, and the model can express a nonlinear stress-strain relation after the cracking of concrete.

The material properties of concrete in the hydration process depend on the volume function that sequentially increases. The stress-strain relationship at a certain point of time is given as the sum of stress-strain relationships of solidified elements at each time step. The global stress at time t_3 shown in Figure 1, for instance, is calculated as follows:

$$\sigma_g(t_3) = dv(t_1 - t_o)\sigma(\varepsilon(t_3)) + dv(t_2 - t_1)\sigma(\varepsilon(t_3) - \varepsilon(t_1)) + dv(t_3 - t_2)\sigma(\varepsilon(t_3) - \varepsilon(t_2)) \quad (1)$$

where $\sigma_g(t_3)$ is the total stress at time t_3; t_i (i=0-2) is the time changing in loading histories; $\varepsilon(t_i)$ is strain at t_i; and $dv(t_{i+1}-t_i)$ is the increment in the volume function.

This constitutive model has two assumptions: (1) the shape of the stress-strain curve on the tension side at each time can be uniquely determined by a volume function; and (2) superposition of the stress-strain curves according to different loading histories is possible on the stress-strain curve determined by the volume function for each time. Assumption (1) specifically means that the strain axis of a stress-strain relationship does not depend on the age and that only the stress axis changes depending on the volume function. Therefore, the tensile stiffness, strength, and the fracture energy of undamaged concrete are assumed to be all expressible by the volume function. Also, (1) and (2) lead to a conclusion that (3) the amount of energy absorption ultimately obtained is nearly constant with or without damage.

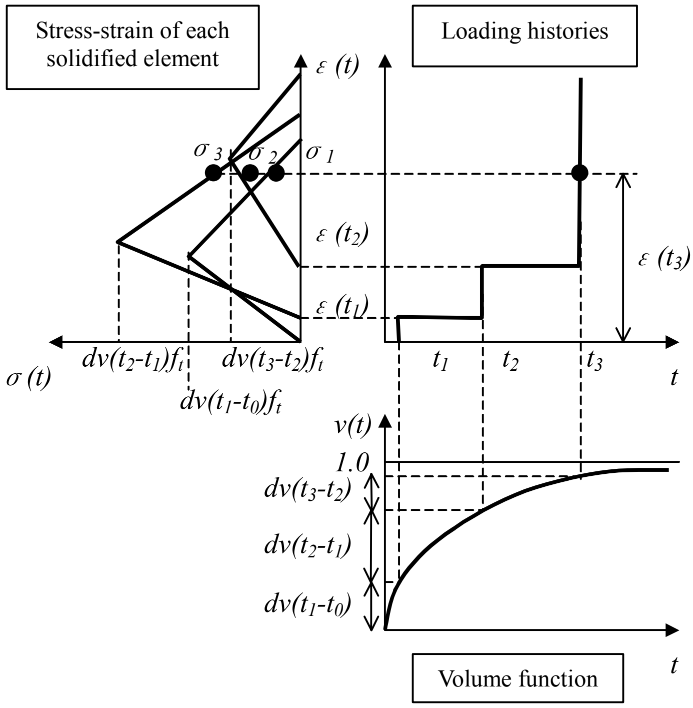

Figure 1. Basic concept on proposed constitutive model.

Table 1. Mix proportions of concrete.

W/C	G_{max}	s/a	Unit content (kg/m^3)				
(%)	(mm)	(%)	*W*	*C*	*S*	*G*	*Ad.*
58.5	15.0	49.8	170	291	893	894	2.91

3 DETERMINATION OF TENSION SOFTENING CURVE ACCORDING TO VOLUME FUNCTION

In this section, the assumption (1) in the previous section is verified through the loading tests at different ages.

3.1 *Outline of experiment*

3.1.1 *Materials*

Table 1 gives the specified mix proportions of concrete used in the tests. The cement, fine aggregate, and coarse aggregate were ordinary portland cement with a density of 3.16 g/cm^3, river sand with a density of 2.59 g/cm^3, and river gravel with a density of 2.57 g/cm^3, respectively. The chemical admixture was an air-entraining and water-reducing agents. The slump and air content of the mixed concrete were 16.7 cm and 6%, respectively.

3.1.2 *Specimens and loading tests*

Beam specimens measuring 100 × 100 × 400 mm were used for flexural tests. A thin plate of 2 mm in thickness was placed in each mold before placing of concrete to make a notch to a depth of 30 mm in the specimen center. Five specimens were fabricated for each series. After being demolded at an age of 1 day, specimens were covered with wetting-cloth, and cured in a thermostatic room at 20°C.

Third-point loading tests were conducted on a loading span of 300 mm. The load and crack mouth opening displacement (CMOD) were measured. Three cylindrical specimens of 100 mm in diameter and 200 mm in height were used for each level of factors for measuring the compressive strength and elastic modulus. The placing and curing procedures were the same as the beam specimens.

3.1.3 *Tested ages*

Flexural tests were conducted at 1, 2, 4, and 28 days (respectively referred to as series 1, 2, 4, and 28) to measure the load-CMOD curve. The specimens were tentatively unloaded to nearly 0 kN when the CMOD reached 0.08, 0.12, 0.18, and 0.24 mm and then reloaded.

3.2 *Test results*

3.2.1 *Strength*

The compressive strength, elastic modulus, and flexural strength at 28 days are 29 MPa, 27 GPa, and 3.5 MPa, respectively.

3.2.2 *Relationship between the shape of load-CMOD curves*

Figure 2 shows the averaged load-CMOD curves at each tested age. Note that the results of three specimens with small scatters out of the five were averaged. The peak load and the area under the load-CMOD curve increase with age. The solid lines in Figure 3 represent the tension softening curves for series 1 and 28 estimated by poly-linear approximation method (Kitsutaka 1997). In regard to these tension softening curves as well, the tensile stress (y-intercept) and the area under the curve (fracture energy) are found to increase with age. The fracture energy at 28 days was 128 N/m.

3.2.3 *Definition of volume function*

Figure 4 and Eq. (2) show the volume function for time dependency in the physical property values formulated and normalized with respect to the 28-day values. However, the compressive strength was excluded from this formulation, as an experimental error was recognized in the data at 4 days.

$$v(t) = \frac{t}{(t+0.6)\times 0.979} \tag{2}$$

Where t is the total time (days). This shows that the development of physical properties, such as the elastic modulus, flexural strength, and fracture energy, are all expressible by this equation.

3.2.4 *Method of determining tension softening curves*

Based on assumption (1) in section 2, a method given in Table 2 was adopted for uniquely determining the bi-linear tension softening curves depending on the volume function, which is based on 1/4 model. Both tensile strength and stress at breaking point depended on the obtained volume function. However, the crack width at breaking point and critical crack width were constant values of 0.12 and 0.012, respectively. As stated above, this method is characterized by the stress changing over time and the crack width being constant independently of age. Figure 3 shows the bi-linear tension softening curves for 1 and 28 days in broken lines calculated by the method given in Table 2. Within the ranges of this study, this method reproduced the shape of the curve to a certain level of accuracy.

Accordingly, it was confirmed that, if the volume function can be specified, then the tensile constitutive model at a given time can be specified.

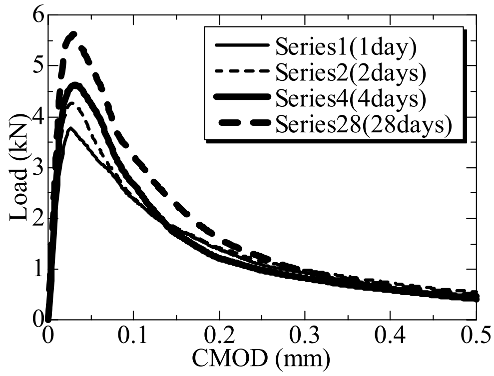

Figure 2. Load-CMOD curves for Series 1,2,4 and 28.

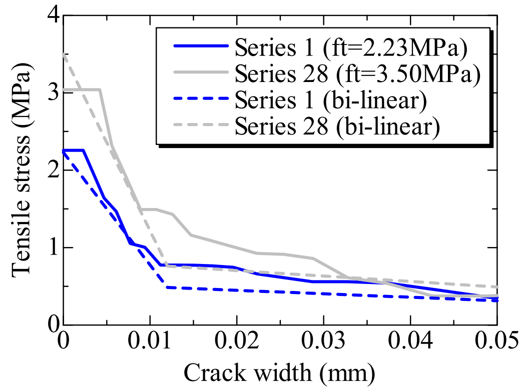

Figure 3. Tension softening curves for Series 1 and 28.

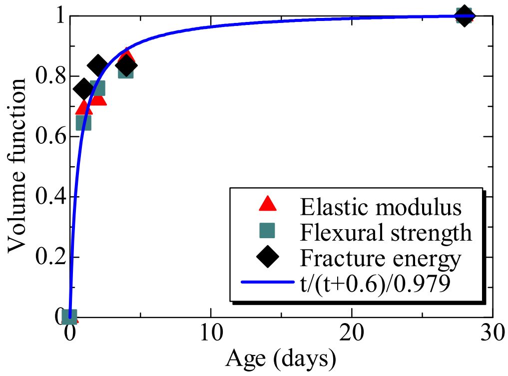

Figure 4. Estimated volume function in the present experiment.

4 EXPERIMENTAL DATA WITH DIFFERENT TEST AGES AND LOADING HISTORIES

4.1 *Outline of experiment*

The materials, specimens, and loading test methods are the same as those described in the previous section.

4.1.1 *Tested ages*

In order to consider the differences in the test age and loading history, the following three groups of tests were conducted: (1) the tests to examine the effect of the degree of damage, (2) the tests to examine the effect of the time of damage, and (c) the tests to examine the effect of repeated damage. Table 3 gives the loading patterns. The specific method for each group is described as follows.

4.1.2 *Tests to examine the effect of the degree of damage*

In order to examine the effect of the degree of damage on the cracking properties after re-curing, loads were applied at an age of 1 day to a CMOD of 0.08, 0.12, 0.18, and 0.24 mm (hereafter referred to as the first loading) as given in Table 3. The specimens were then re-cured until re-loading at an age of 28 days (hereafter referred to as the second loading). For instance, the series $1^{0.08}$-$28^{0.5}$ is loaded to a CMOD of 0.08 mm at 1 day, unloaded, re-cured, and re-loaded to failure at a total age of 28 days (expressed as 0.5 mm for convenience). It should be

Table 2. Determination rules for bi-linear tension softening curves (1/4 model basis).

Parameters	Determination rules
Tensile strength	According to the volume function (time-dependent)
Stress at breaking point	1/4 of the tensile strength (time-dependent)
Crack width at breaking point	Constant value (0.012mm)*
Critical crack width	Constant value (0.12mm)*

*These values were obtained from the test results at 28 days (through inverse analysis)

Table 3. Loading patterns.

Series	Testing Ages			
	1 day	2 days	4 days	28 days
$1^{0.08}$-$28^{0.5}$	1st(0.08) →			2nd(fract.)
$1^{0.12}$-$28^{0.5}$	1st(0.12) →			2nd(fract.)
$1^{0.18}$-$28^{0.5}$	1st(0.18) →			2nd(fract.)
$1^{0.24}$-$28^{0.5}$	1st(0.24) →			2nd(fract.)
$4^{0.08}$-$28^{0.5}$			1st(0.08) →	2nd(fract.)
$4^{0.12}$-$28^{0.5}$			1st(0.12) →	2nd(fract.)
$4^{0.18}$-$28^{0.5}$			1st(0.18) →	2nd(fract.)
$4^{0.24}$-$28^{0.5}$			1st(0.24) →	2nd(fract.)
$1^{0.08}$-$2^{0.5}$ *	1st(0.08) →	2nd(fract.)		
$1^{0.08}$-$2^{0.12}$-$4^{0.5}$	1st(0.08) →	2nd(0.12) →	3rd(fract.)	
$1^{0.08}$-$2^{0.12}$-$28^{0.5}$	1st(0.08) →	2nd(0.12) →		3rd(fract.)
$1^{0.08}$-$2^{0.12}$-$4^{0.18}$-$28^{0.5}$	1st(0.08) →	2nd(0.12) →	3rd(0.18) →	4th(fract.)

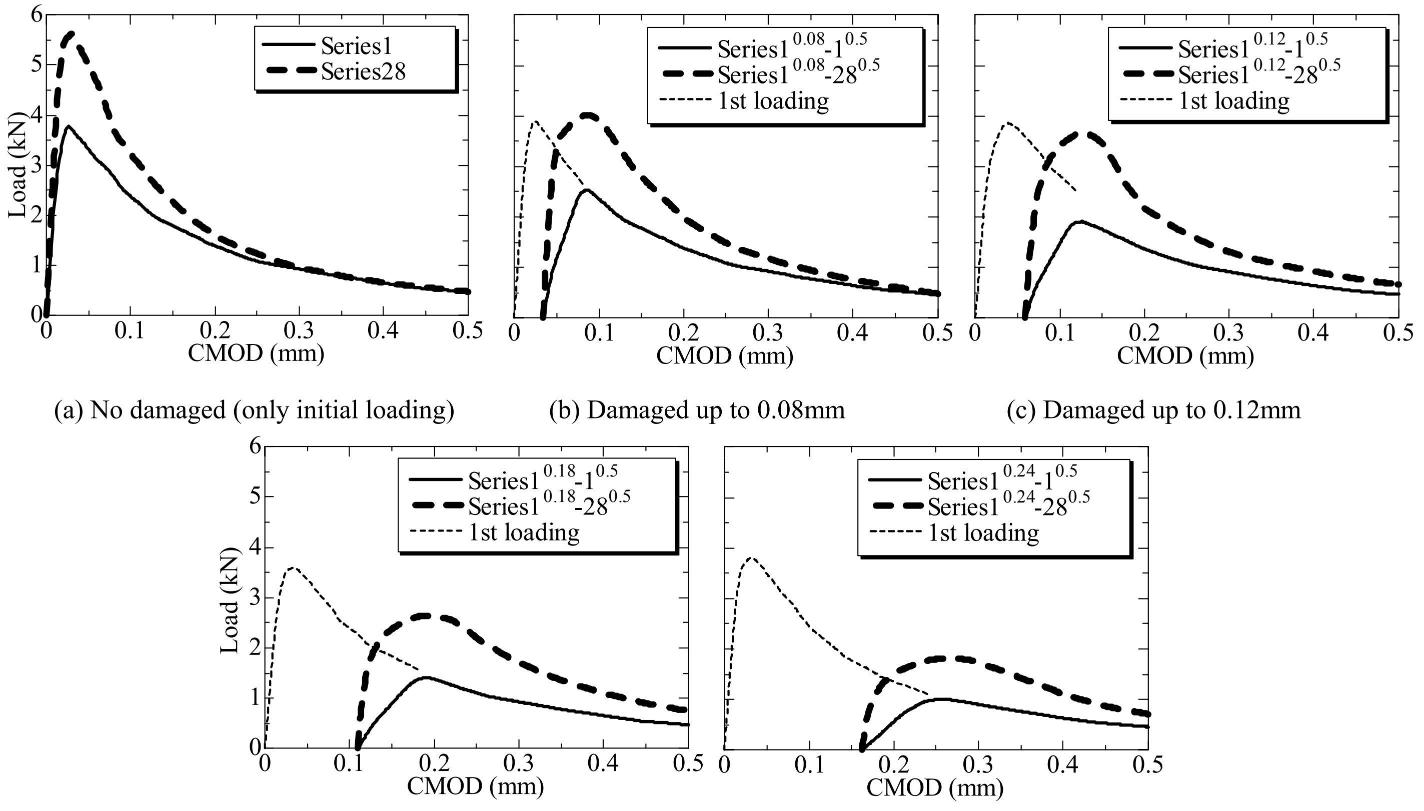

(a) No damaged (only initial loading) (b) Damaged up to 0.08mm (c) Damaged up to 0.12mm

(d) Damaged up to 0.18mm (d) Damaged up to 0.24mm

Figure 5. Load-CMOD curves (first loading: 1day, second loading: 28days).

noted that re-curing was same conditions as initial curing (covered with wetting-cloth, in a thermostatic room at 20°C).

4.1.3 *Tests to examine the effect of the time of damage*

The first loading was applied at 4 days to a CMOD of 0.08, 0.12, 0.18, and 0.24 mm, and after re-curing, the second loading was applied at 28 days as given in Table 3 to investigate the effect of the time of damage on the cracking properties after re-curing.

4.1.4 *Tests to examine the effect of repeated damage*

As given in Table 3, the first loading was applied to the specimens at 1 day to a CMOD of 0.08 mm, and

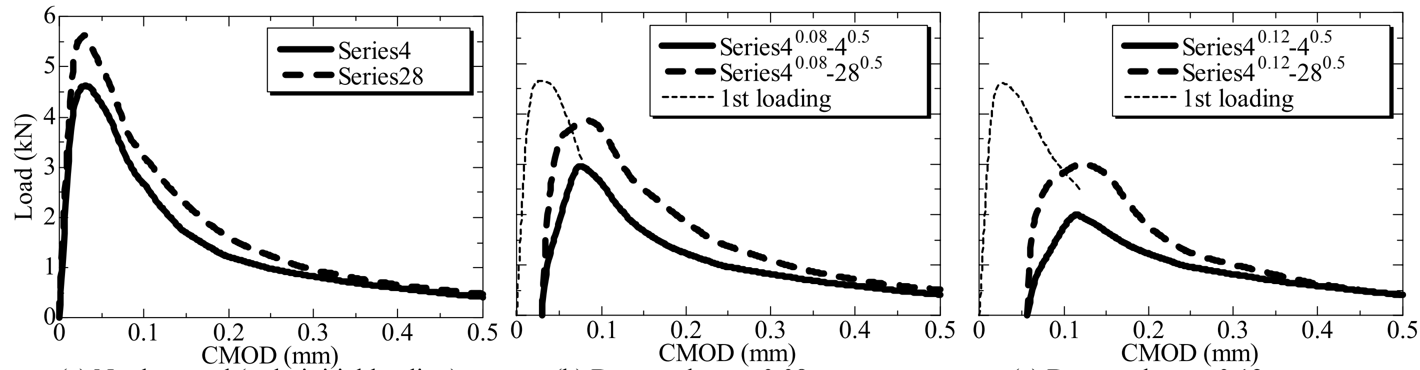

(a) No damaged (only initial loading) (b) Damaged up to 0.08mm (c) Damaged up to 0.12mm

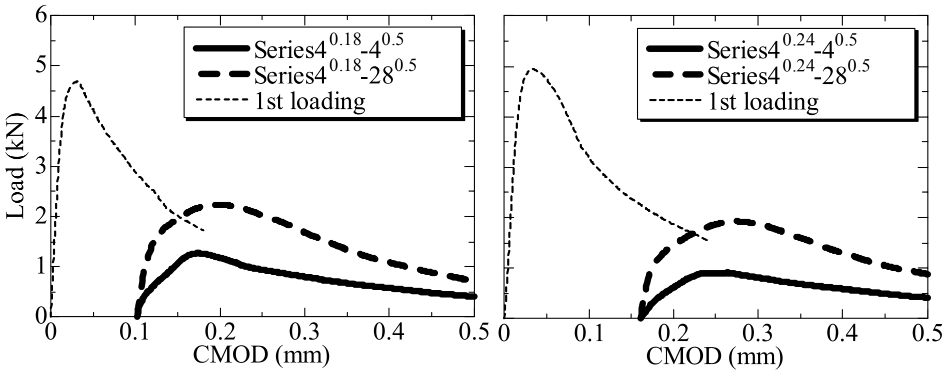

(d) Damaged up to 0.18mm (d) Damaged up to 0.24mm

Figure 6. Load-CMOD curves (first loading: 4day, second loading: 28days).

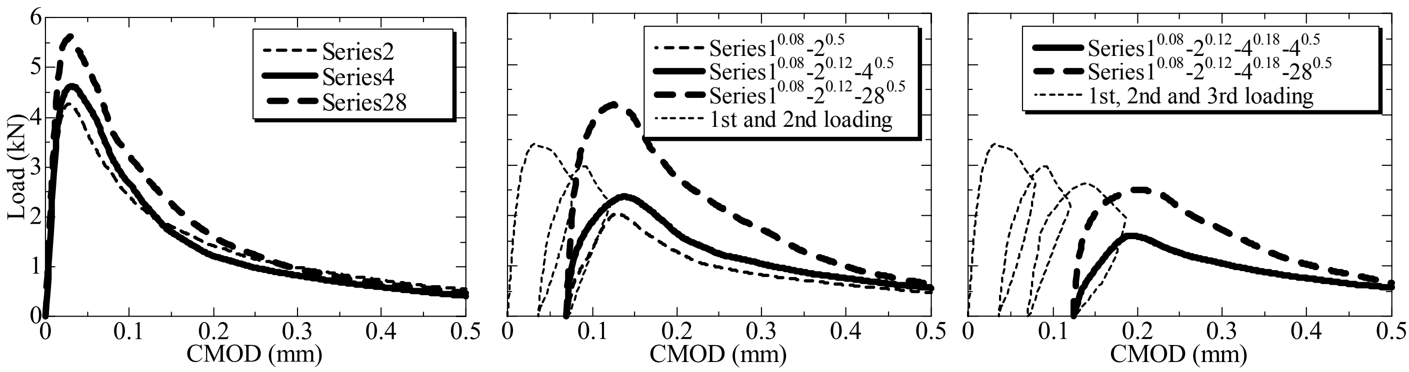

(a) No damaged (only initial loading) (b) Repeated damage up to 0.12mm (c) Repeated damage up to 0.18mm

Figure 7. Load-CMOD curves (repeated damage series).

after re-curing, the second loading was applied at 2 days to a CMOD of 0.12 mm. After further curing, the third loading was applied at 4 or 28 days, or the third and fourth loading were applied at 4 and 28 days, again with curing in between.

4.2 *Test results*

4.2.1 *Effect of the degree of damage*

Figure 5 shows the load-CMOD curves of specimens damaged to a CMOD of 0.08 mm at 1 day, re-cured, and subjected to the second loading at 28days. Five specimens were tested for each series, and the curves of three specimens with the smaller scatters were averaged, similarly to the section 3. The results of undamaged specimens are also shown in Figure 5(a) for reference.

Even with the damage due to the first loading, the peak load and the area under the curve also increase as the age of the second loading increases. However, both peaks of this series undergoing the first and second loading are smaller than those of specimens with no damage shown in Figure 5(a). Also, a higher degree of damage under the first loading tends to lead to a smaller peak load under the second loading at 28 days. This is presumably because the damage accumulated under the first loading adversely affects subsequent hydration.

4.2.2 *Tests to examine the effect of the time of damage*

Figure 6 shows the averaged load-CMOD curves of specimens subjected to the first loading at 4 days, re-cured, and re-loaded at 28 days. The results of un-

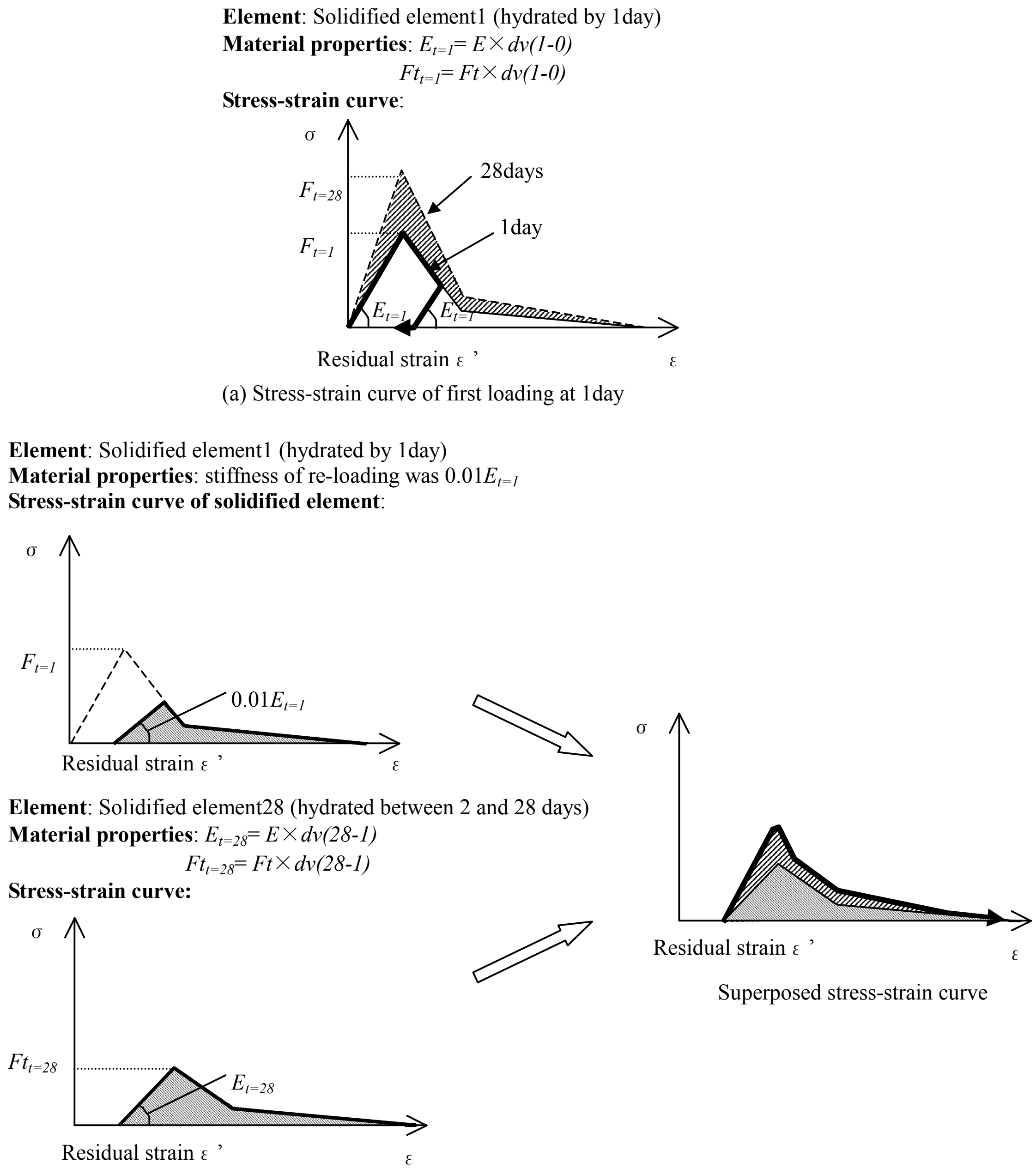

(a) Stress-strain curve of first loading at 1day

(b) Superposed stress-strain curve of second loading at 28 days

Figure 8. Example of superposed stress-strain curves focusing on each solidified element (first loading: 1day, second loading 28days).

damaged specimens are also shown in Figure 6(a) for reference. The series subjected to the first loading at 1 day were already shown in Figure 5.

The first loading at an earlier age to a lower degree of damage tends to lead to a higher peak load under the second loading and a larger area under the curve. However, the peak load is lower than those of undamaged specimens in all series.

4.2.3 *Tests to examine the effect of repeated damage*

Figure 7 shows the averaged load-CMOD curves obtained from specimens subjected to repeated damage. The peak load and the area under the load-CMOD curve of repeatedly damaged specimens are also found to increase with age. However, the peak loads are lower than those of undamaged specimens (see Fig. 7 (a)).

5 ANALITICAL VERIFICATION REGARDING SUPERPOSITION OF STRESS-STRAIN CURVES

In this section, numerical analyses are conducted to verify the superposition of stress-strain curve specified using volume function, as described in assumption (2) in section 2.

5.1 *Volume function*

The equation (2) was used as the volume function to express the levels of various physical properties developing with age. The analytical material characteristic values (compressive strength, tensile strength, and elastic modulus) at 28 days multiplied by the

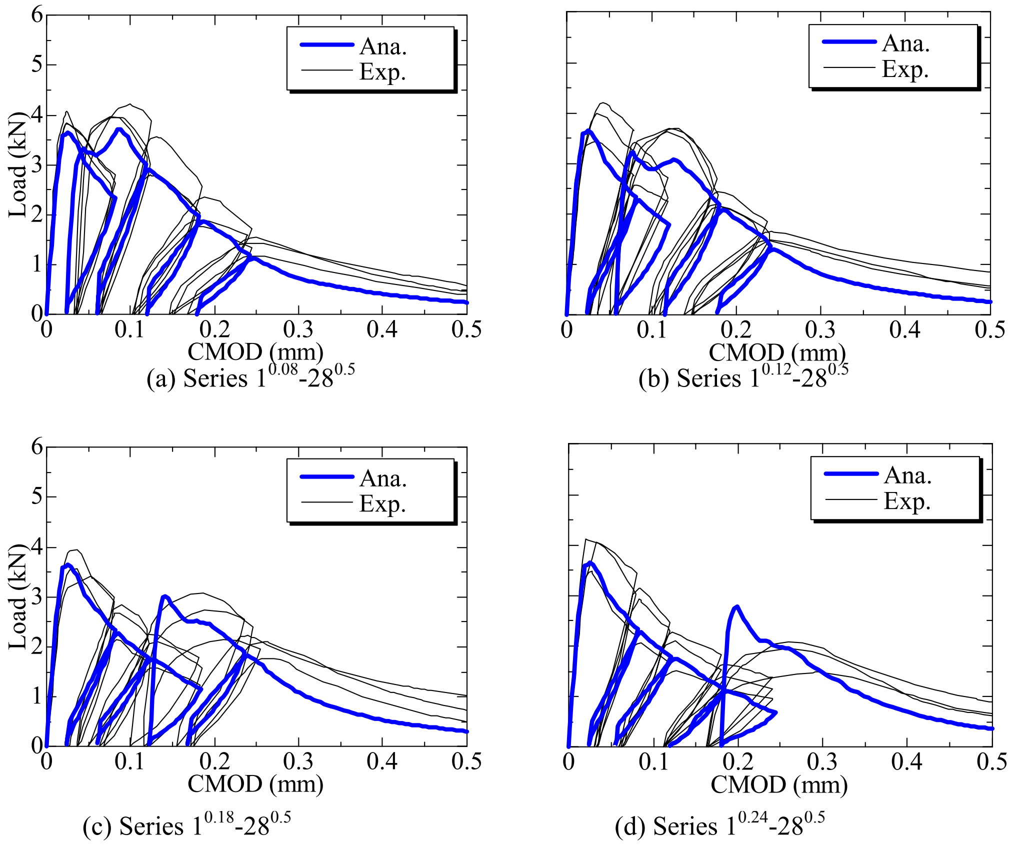

(a) Series $1^{0.08}$-$28^{0.5}$ (b) Series $1^{0.12}$-$28^{0.5}$

(c) Series $1^{0.18}$-$28^{0.5}$ (d) Series $1^{0.24}$-$28^{0.5}$

Figure 9. Analytical load-CMOD curves (first loading: 1day, second loading: 28days).

volume function were used as the material characteristic values at each age.

5.2 *Tension softening curves (stress-strain curves) and their superposition*

The tension softening curve at each time step was calculated in stress-strain levels using the volume function values as shown in Figure 1 and superposed to formulate the overall stress-strain curve by the method given in Figure 8. Regarding the second loading, for instance, residual stress-strain curve of solidified element 1 and newly generated stress-strain curve of solidified element 28 due to hydration by re-curing were superposed at residual strain level.

5.3 *Rigid-Body-Spring Model (RBSM)*

The Rigid-Body-Spring Model(RBSM) proposed by Kawai (1978) was used to reproduce the analytical mechanical behavior. The mesh dependence of cracking was reduced by dividing the concrete into random cells(Bolander & Saito 1998). Each concrete cell has three degrees of freedom, and also has a normal spring (kn), shear spring (ks), and rotational spring (kq) at the cell boundaries.

5.4 *Analytical results*

Figures 9 and 10 show the analysis and test results of specimens subjected to the first loading at 1 and 4 days, respectively, and second loading at 28 days. The shapes of the overall load-CMOD curves are roughly well-estimated, including the behavior in which the peaks under the second loading are increased by re-curing after the first loading.

According to the analysis, the total energy consumed by the time of fracture at 28 days is nearly constant with or without the damage and independently of the damage history. As shown in Figure 9 (d), the behavior under the first loading is basically well-estimated, but the load and energy absorption under the second loading are reproduced as being slightly greater than the test values. This is presumably because the damage to a high degree under the first loading (approximately 0.24 mm in this study) adversely affects the subsequent hardening process of specimens.

Figure 11 shows the analyzed and tested values of specimens subjected to repeated loading. The overall behavior is again well-reproduced, proving that it is possible to estimate the overall behavior by superposing the stress-strain curve for each age.

6 CONCLUSIONS

In this study, flexural loading tests on specimens with different loading histories were conducted to verify the validity of a constitutive model capable of incorporating the hardening process and loading histories of concrete. The major conclusions are summarized as follows:

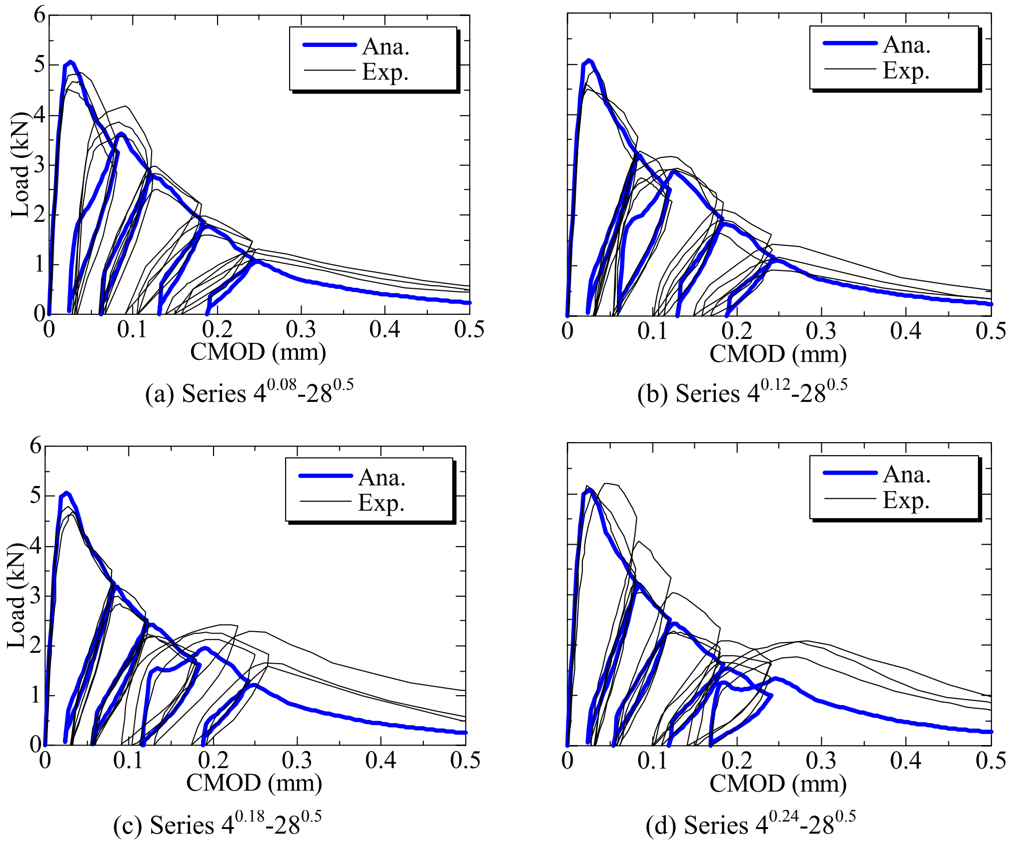

Figure 10. Analytical load-CMOD curves (first loading: 4days, second loading: 28days).

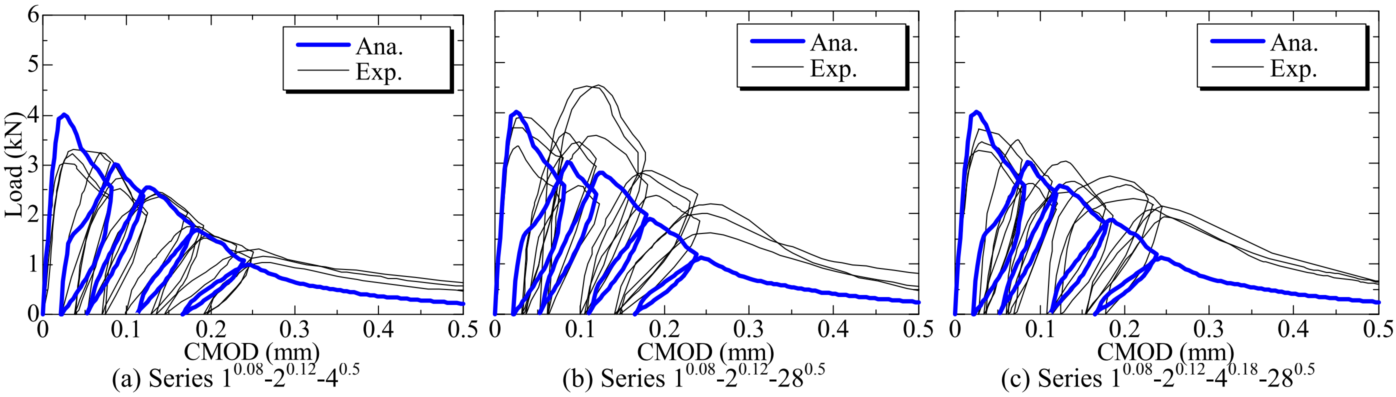

Figure 11. Analytical load-CMOD curves (repeated damage series).

(1) A method of specifying the shape of a bilinear tension softening curve using a volume function produced from time-dependent changes in various material properties was proposed, with its validity being verified by comparison with test results.
(2) A technique of superposing a stress-strain curve specified using a volume function for each time step was analytically verified using the RBSM. This technique roughly reproduced the experimental load-CMOD curves, proving its validity.

The authors intend to pursue a method of specifying a more precise volume function, as well as to investigate the unloading path of the model, the effect of creep, and the applicability to other types of concretes, to develop a more generalized constitutive model.

REFERENCES

Bazant, Z. P. and Prasannan, S. 1989. Solidification theory for concrete creep I: Formulation, *Journal of Engineering Mechanics*, ASCE, 115(8): 1691-1703

Bolander, J. E. and Saito, S. 1998. Fracture analysis using spring networks with random geometry. *Engineering Fracture Mechanics*, 6: 569-591

Ishikawa, Y, Kunieda, M., Srisoros, W. and Tanabe, T. 2005. Modeling of uni-axial constitutive law in early age concrete based on solidification concept, *Proc. of Concreep7*, 393-398

Kawai, T. 1978. New discrete models and their application to seismic response analysis of structure, *Nuclear Engineering and design,*48: 207-229

Kitsutaka, Y. 1997. Fracture parameters by poly-linear tension softening analysis, *Journal of Engineering Mechanics*, ASCE, 123(5): 444-450

Srisoros, W. (2006). Development of time-dependent structural analysis method and constitutive model for concrete structures, Ph.D Thesis, Nagoya University